Conceptual Design of a Flying-V Aircraft Family

Oosterom, W.J.; Vos, Roelof

DOI
10.2514/6.2022-3200

Publication date
2022

Document Version
Final published version

Published in
AIAA AVIATION 2022 Forum

AIAA AVIATION Forum
June 27-July 1, 2022, Chicago, IL & Virtual
AIAA AVIATION 2022 Forum

10.2514/6.2022-3200

Conceptual Design of a Flying-V Aircraft Family

W.J. Oosterom* and R. Vos†
Delft University of Technology, Kluyverweg 1 2629HS Delft, The Netherlands

The Flying V is a flying-wing aircraft, which promises a 20% reduction in fuel consumption compared to a conventional twin-aisle commercial transport. The passenger cabin, cargo hold and fuel tanks are all integrated into a highly-swept, cranked wing. This study presents the conceptual design of a three-member family of Flying-V aircraft with maximal commonality between the family members. A design process is proposed to automate the synthesis process of the aircraft family comprising all relevant disciplinary analysis methods. A vortex-lattice method is employed to study the aerodynamic characteristics of the aircraft, enhanced with a viscous drag prediction method to estimate the lift-to-drag ratio. Weight of the aircraft is estimated using a combination of empirical and analytical methods. A constrained optimization algorithm is employed that minimizes fuel consumption, ensuring commonality in terms of design-variable values between family members. Comparing the resulting two largest family members to their conventional twin-aisle counterparts shows a 20% and 22% reduction fuel burn, respectively. The smaller two family members feature 100% commonality with the largest family member allowing for further reduction in fuel consumption if this constraint is relaxed. Driving parameters in Flying-V family design are the center-of-gravity excursion during flight, the wing span and the fuel tank volume.

Nomenclature

b	= wing span (m)	E	= endurance (s)
b_{outer}	= outer wing span (m)	f	= form factor (-)
c	= chord length (m)	H_1	= oval crown height (m)
c'	= normalized planform chord length (-)	H_3	= oval keel height (m)
C_D	= drag coefficient (-)	L	= lift force (N) or length (m)
C_f	= skin friction coefficient (-)	R	= range (m)
C_L	= lift coefficient (-)	S	= wing (reference) area (m^2)
C_{L_α}	= lift coefficient slope (1/rad)	V	= velocity (m/s)
C_{l_β}	= lateral stability coefficient (1/rad)	W	= weight (N)
C_{n_β}	= directional stability coefficient (1/rad)	α	= angle of attack (deg)
c_T	= specific fuel consumption (N/N/s)	λ	= taper ratio (-)
D	= drag force (N)		

I. Introduction

MULTIPLE sizes of one transport aircraft are often designed to offer a range of aircraft suitable for different missions and payloads: an aircraft family. Making a family out of tube-and-wing aircraft is relatively straightforward: stretching or shrinking the tube allows for more or less payload capacity, respectively. Sometimes this is accompanied by small modifications to the wing, such as a chord extension (A321). Finally, the engine is either exchanged for a different engine or the same engine with a different thrust rating. Such a family of aircraft is attractive to limit development and nonrecurring cost per family member, as many components are shared between the individuals. The same holds for the operator whose operating cost are lower due standardization between the various family members within their fleet [1]. On the other hand, designing a family also has drawbacks. For example: the heaviest family member dictates the required size of the wing and strength of the wing box. This implies that smaller family members fly their operational

*MSc student, Faculty of Aerospace Engineering.
†Assistant Professor, Faculty of Aerospace Engineering, R.Vos@tudelft.nl, AIAA Associate Fellow.

life with an over-sized wing in terms of dimension and weight leading to more fuel burn. In other words, the higher the commonality between the individual members, the higher the "commonality penalty."

Flying-wing airplanes, such as the YB-35, B-2 or blended wing body (BWB) are more difficult to design as an aircraft family. As the wing is often tapered and swept, add a simple "plug" that can stretch the payload bay also affects all other wing aspects. Although challenging for the BWB, Liebeck states "commonality may be the key to provide the incentive and courage to proceed to develop this new airplane concept." ([2] p. 4) According to Liebeck, commonality in a family of two blended wing body designs can offer a 23% and 12% reduction in nonrecurring and recurring cost respectively [2]. On the contrary, Michael Sinnett, former vice-president of Product Development and Future Airplane Development at Boeing, stated in 2018 that a BWB does not lend itself to a stretch or shrink. "You take the most expensive part of the airplane, the non-constant section, and growing it in a non-constant way, or shrinking it in a non-constant way. It's really hard."*

The Flying V is a flying-wing transport aircraft with passengers, cargo and fuel in the wing (1). It consists of a highly-swept inner wing, which has most of the volume, and an outer wing with reduced sweep angle [3]. Contrary to the BWB, the inner wing of the Flying V does allow it to be stretched or shrunk in a relative straightforward manner: by adding or removing constant-section wing plugs. This makes the Flying V different from other flying-wing designs and improves its commercial potential significantly. Prior studies have shown that the Flying V can have a 15% improvement in aerodynamic efficiency [4] due to its reduced wetted area. Unpublished studies performed by TU Delft and Airbus GmbH have also shown that the span loading of the Flying V is reduces the structural weight significantly. Furthermore, the fact that a Flying V family uses wing plugs to increase its payload capacity has a potentially beneficial side effect: the wing grows with increased take-off weight keeping the wing loading fairly constant between the family members. In other words, the largest family member does not dictate the dimension of the wing for a Flying-V aircraft family.

Fig. 1 Artist impression of the the Flying V configuration

For transport aircraft, two main family design principles exist. Sequential family design aims at designing a baseline product and designing several derivatives from this product. The Boeing 747 family is an example of a sequentially designed aircraft family. Simultaneous family design optimizes multiple products at once, and has been proven to yield better results than sequential design. For instance, Willcox and Wakayama found that simultaneously designing a family of BWB aircraft led to a small reduction of 0.2% in take-off weight compared to a sequential design procedure [5]. Also, the reference aircraft family for the Flying-V, the Airbus A350 family, has also largely been designed simultaneously [6]. The question is whether these envisioned benefits of the Flying V materialize when one performs the simultaneous design of the Flying-V aircraft family.

To study this, we perform a simultaneous family design optimization for the Flying V, where we enforce maximum commonality between the individual family members. Here, commonality is used as a concept to describe amount of equal components between the members of the Flying-V family. Commonality is maximized by defining the majority of the design variables describing an aircraft to be equal between aircraft family members. Variable-based commonality methods, often based on the approach of Messac et al. [7], automatically select the scaling variable(s). However, such an approach is not considered suitable for the specific problem at hand. Variable-based commonality models do not include any information on cost or complexity of changing one variable instead of another, such that a manual selection of the scaling variable is deemed the most viable option for this research. Parameters describing the shape of the Flying-V are related to the cross-section of the cabin and wing and the planform of the wing, of which only the length of the

*https://leehamnews.com/2018/04/03/dont-look-for-commercial-bwb-airplane-any-time-soon-says-boeings-future-airplanes-head/ [cited on 12-5-2020]

untapered part of the wing is found applicable for scaling, such that the benefits of commonality can be captured. Other parameters, such as the width of the cabin or the outer wing span are held equal between the individual family members to maximize commonality.

Figure 2 visualises the common components between the family members, as well as plugs to lengthen the untapered part of the aircraft wing and the fuselage structure with the engine and landing gear attached. The length of the fuselage[†] plugs for the different aircraft variants are based on the difference in the total length of the fuselage of the aircraft as well as on the difference in engine and landing gear location. The landing gear location determines the location of the entire fuselage component it is connected to. The smallest variant of the Flying-V imposes a constraint on the length of the tapered fuselage part, since the engine should be attached to the untapered cabin to allow the insertion of frames aft of the engine for larger aircraft.

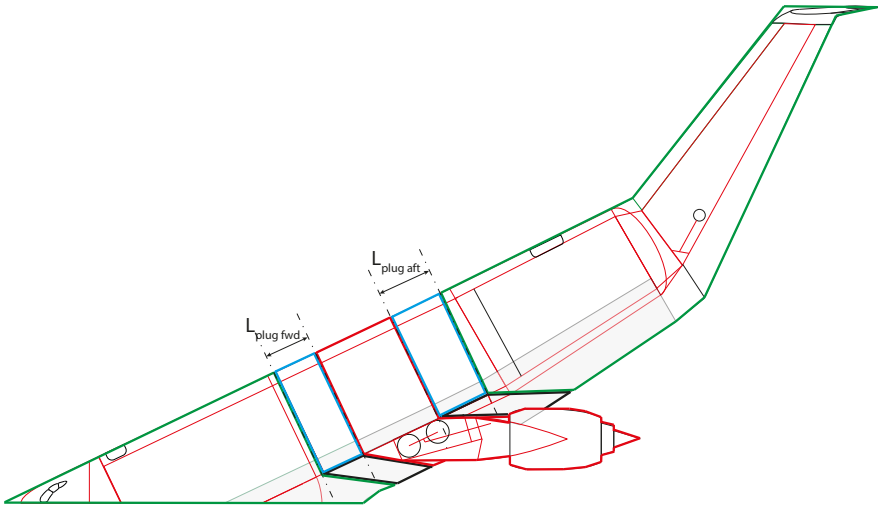

Fig. 2 Components of each aircraft family member. Similar components (green), fuselage plugs (blue) and the moving section with the engine and landing gear (red). The floor plan and component locations are only indicative.

Enforcing maximal commonality, this implies that smaller family members have 100% commonality with their larger relatives. The commonality penalty that is a obtained when performing simultaneous family design with maximal commonality comprises two aspects. First, a weight penalty due to the selection of the strongest (and therefore heaviest) structural member for the complete aircraft family. This penalty can be easily quantified by comparing equal aircraft designs with and without the constraint of using the heaviest component or thickest structural member. The second penalty is due to the selection of common values for the design variables for the complete aircraft family, i.e. optimizing design variables for a family of aircraft rather than for an individual aircraft member.

The question to be answered is: how does the fuel-burn performance of the Flying-V aircraft family compare to a tube-and-wing aircraft family if both are designed for the same top-level requirements and the former is designed for maximal commonality using a simultaneous design approach? Associated questions that are answered are: what is the commonality penalty in terms of fuel-burn performance, and what are the driving top-level requirements in an optimized Flying-V family design? To answer these questions, a simultaneous family design and synthesis method is defined in section II. In section III this method is verified and its results are validated. The results of the family design are presented and discussed in section IV. Finally, section V concludes and provides directions for future research.

II. Methodology

Previous studies on the Flying-V have been using the ParaPy framework, a Knowledge-Based Engineering (KBE) environment programmed in Python[‡] of which the characteristics are extensively discussed by La Rocca [8]. This framework is also employed in this study. The optimization architecture to size a single aircraft is visualized in Figure 3.

[†]In this context, the word "fuselage" is used of the part of the wing structure that is pressurized comprising the cabin and the cargo hold.

[‡]`https://www.parapy.nl/` [cited on 23-9-2020]

The white blocks in the top row of this diagram show the input to the method in terms of initial values of the design variables, fixed constraint values, or constants. The design variables describing the geometry (e.g. H, L_i, etc.) are fully explained in Section II.A. The analysis modules are located on the diagonal of the diagram. The grey blocks in the diagram represents the data that migrates as output from one analysis module the input of another analysis module. Two loops can be distinguished within this process. The inner loop is a multidisciplinary analysis (MDA) loop that converges when the fuselage weight does not change with more than 1% between two iterations. The outer loop optimizes the different variables describing the aircraft using fuel burn as minimization objective while satisfying top-level aircraft requirements (TLRs) and constraints. The aerodynamic analysis, weight estimation method, fuel burn analysis and optimization are described Sections, II.B, II.C, and II.D, respectively. The optimisation algorithm used to perform the optimization procedure is the Differential Evolution (DE) algorithm, implemented in SciPy [§] and described by Storn and Price [9].

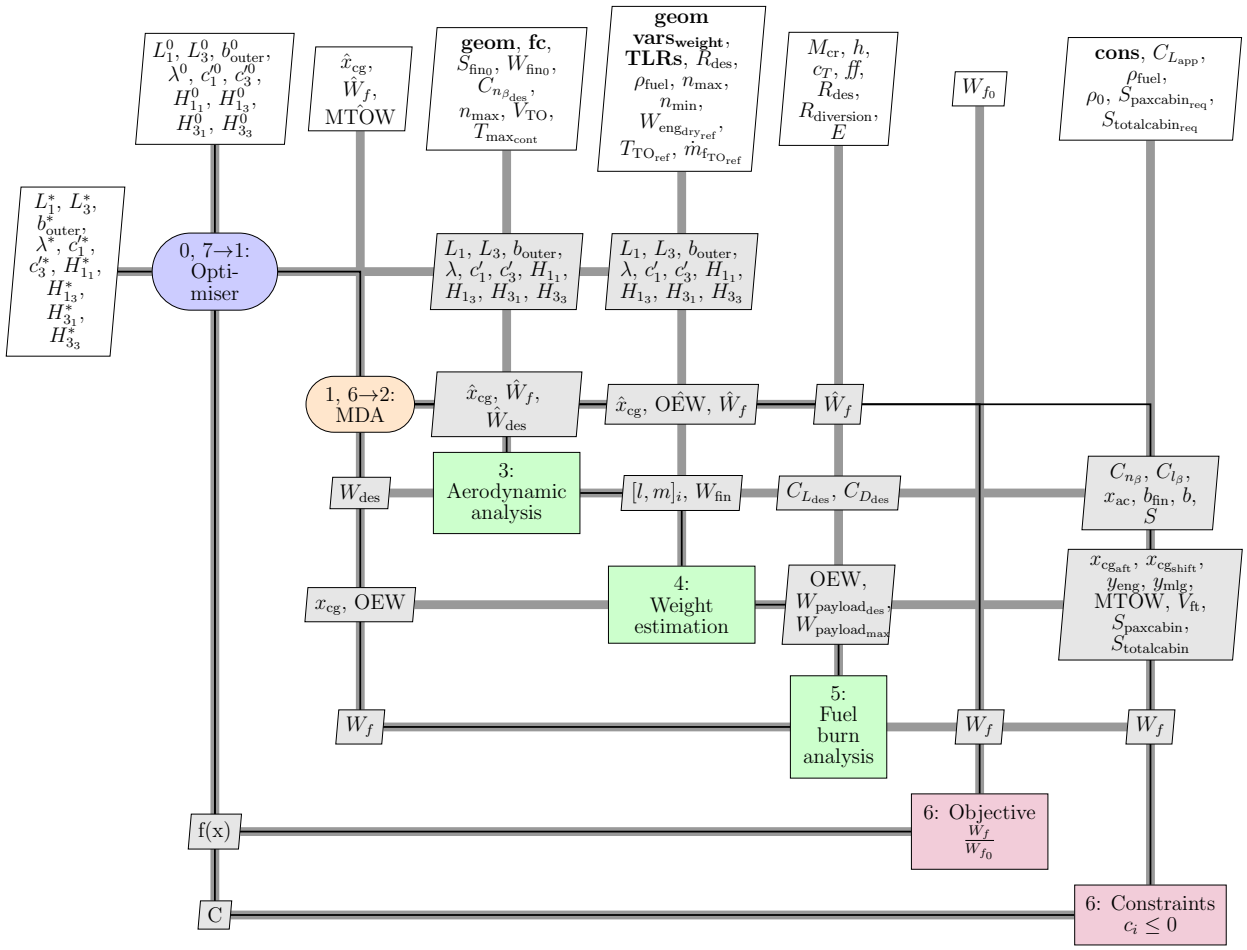

Fig. 3 Process flow of the design and optimization method for a single airplane. TLRs are top-level requirements provided in Table 6, cons are constraint values provided in Table 7, geom are fixed variables describing the Flying-V shape provided in Table 14, vars$_{\text{weight}}$ are inputs to the weight estimation model provided in Table 15 (see appendix) and fc are standard atmospheric conditions.

To perform the family design, the MDA process of Fig. 3 is performed for all members in the family. In this study, three family members are considered, therefore the MDA process is performed three times as can be seen in Figure 4. Note that the geometrical input to all three MDA processes is largely the same, except for the length L_1, which is the length of the constant-cross-section fuselage. Compared to the single-aircraft optimization, the objective has now

[§] `https://docs.scipy.org/doc/scipy/reference/generated/scipy.optimize.differential_evolution.html` [cited on 26-11-2020]

changed to minimize the sum of the fuel burn of all three aircraft.

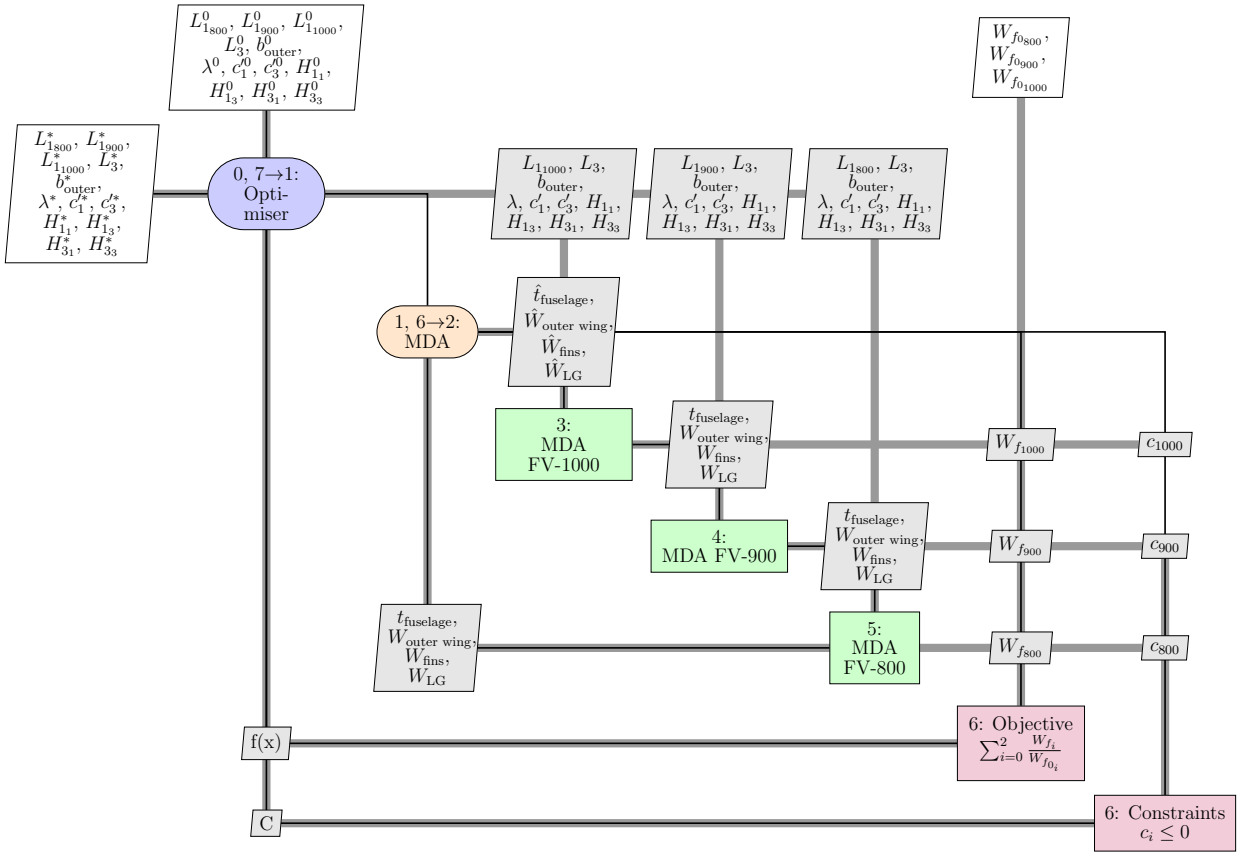

Fig. 4 Process flow of the aircraft family optimization method.

A. Parametrization and Flying-V Family Design

Hillen [10] provides a parametrization of the Flying-V, which is visualized in Figure 5. During optimization of a single aircraft or a family of aircraft, variables indicated in green and red are varied whereas variables indicated in black are fixed. Fixed variables, such as the width of the cabin w_H, are not varied to limit the scope of this research and to enable comparison of the results with earlier Flying-V studies. Sections 4 and 5 on the Flying-V planform are airfoils described by CST coefficients.

All variables indicated in green in Figure 5 are set equal between aircraft family members by the optimizer. The length of the untapered cabin L_1, indicated in red, is the only design variable that is allowed to differ between the family members. The length of the fuselage plugs for the different aircraft variants (as shown in Figure 2) is based on the difference in L_1 as well as on the difference in engine and landing gear location. The landing gear location is determined as described in Section II and determines the location of the fuselage trunk it is connected to. The smallest variant of the Flying-V imposes a constraint on the length of the tapered cabin part, since the engine should be attached to the untapered cabin to allow the insertion of frames aft of the engine for larger aircraft. Hence, the tapered cabin length L_3 is constrained at a maximum of 11 m.

The structure of the Flying V is based on stiffened shell elements. The thickness of all common fuselage structural members should be sufficient to carry the loads of the most heavily loaded variant. This is ensured by selecting the highest thickness for every shell element from all aircraft variants. Similarly, the heaviest variants for the winglets, landing gear, APU and outer wing are used on all aircraft family members. The weight of the systems, furniture and operational items are assumed to scale with input parameters such as the takeoff weight and cabin length and are therefore unique for each family member. The location of the nose gear and the size of the elevons are set to be the same for all variants.

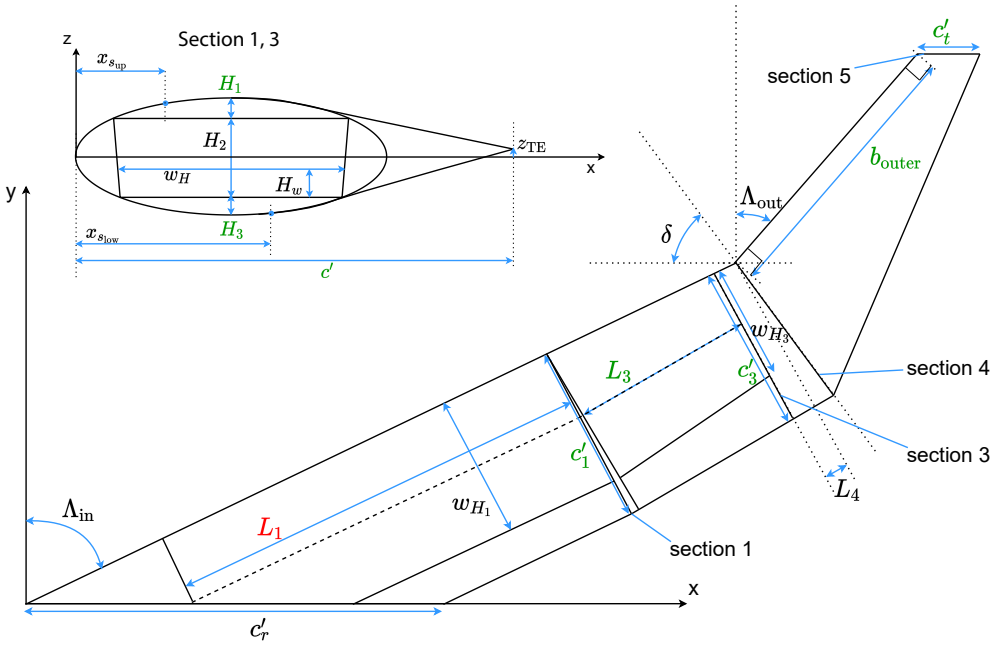

Fig. 5 Parametrisation of the Flying-V planform and cross section. Fixed variables are shown in black and design variables in green. The unique variable between family members, L_1, is indicated in red. Fixed variables are explained in Table 14.

B. Aerodynamic Analysis

The vortex-lattice method AVL is used for aerodynamic analysis of the Flying V. It has low computational cost, direct integration in the ParaPy framework, computes stability derivatives, and computes sectional lift and moment distribution. The Flying-V model is approximated by modeling only the wing-fuselage structure in AVL, neglecting the engines and winglets. The fins are sized for directional static stability, one engine inoperative condition at takeoff and landing in maximum crosswind condition, adopting the procedure of Faggiano et al. [4]. The viscous drag of the winglets is assumed to balance the reduction in lift-induced drag due to the winglets.

A two-component drag polar is assumed to represent the aerodyanmic performance of the aircraftaccording to:

$$C_D = C_{D_0} + \frac{C_L^2}{\pi A e} \tag{1}$$

The Oswald factor e is found by running AVL at an estimated design lift coefficient $C_{L_{\text{des}}}$ and solving Equation 1 for this condition:

$$C_{L_{\text{des}}} = \frac{W_{\text{des}} g}{\frac{1}{2}\rho V^2 S} \tag{2}$$

where g is the gravitational acceleration and ρ is the density at cruise altitude. As shown in Figure 3, the design cruise weight W_{des} is iteratively determined within the MDA loop.

The zero-lift drag consists of the following three components::

$$C_{D_0} = C_{D_{0_{\text{wing}}}} + C_{D_{0_{\text{pylons}}}} + C_{D_{0_{\text{nacelles}}}} \tag{3}$$

Zero-lift drag of the wing is computed using the strip method based on Raymer [11], which has been used before by Faggiano and Vos, neglecting lift-related profile drag but accounting for skin friction and pressure drag [4]. For the nacelle drag, the method of Raymer is employed, which uses a form factor based on the diameter-to-length ratio of the nacelle [11]. Finally, the zero-lift drag coefficient of the pylons $C_{D_{0_{\text{pylons}}}}$ is estimated to be $3 \cdot 10^{-4}$ based on the study by Bourget [12].

C. Weight Estimation Method

The takeoff weight W_{TO} of the aircraft consists of the following components.

$$W_{\text{TO}} = W_{\text{OEW}} + W_{\text{payload}} + W_{\text{fuel}} \tag{4}$$

The operating empty weight W_{OEW} is the sum of many component weight groups:

$$W_{\text{OEW}} = W_{\text{LG}} + W_{\text{propulsion}} + W_{\text{oper items}} + W_{\text{furniture}} + W_{\text{systems}} + W_{\text{structure}} \tag{5}$$

The systems, operational items, landing gear, engine, cabin provisions and payload items do not differ much from conventional aircraft configurations. The weight of these elements is estimated using the Class II weight estimation method of Torenbeek [13]. Note that the dry engine weight for the Flying-V family members is determined based on engines of the reference aircraft family, scaling down the dry weight of the engines proportionally to the takeoff weight to account for the reduced takeoff weight of the Flying-V aircraft. A fundamental assumption of this scaling is a similar thrust-to-weight ratio between the reference aircraft and the Flying-V.

The structural weight of the Flying V is computed using a combination of analytical and empirical methods. The analytical models are sensitive to the geometry and structural topology of the Flying V components as well as to the loads that are imposed to the geometry. The geometry of a Flying-V is modeled as a combination of simplified components shown in Fig. 6. The outer wing is modeled as a box structure comprising a front spar, an aft spar, an upper skin panel and a lower skin panel. The oval fuselage structure is modeled according to Vos and Hoogreef [14] with skin panels and an interior box structure to sustain the pressurization loads without large deformations. The so-called "symmetry parts" are not modeled, since a part of equal dimensions is included in the simplified oval fuselage geometry, as indicated by the blue overlapping parts. Note that the spars of the outer wing do not align with the oval fuselage structure of the inner wing, which is a direct result of the assumption to model the geometry of the Flying-V as a combination of simplified and separate components.

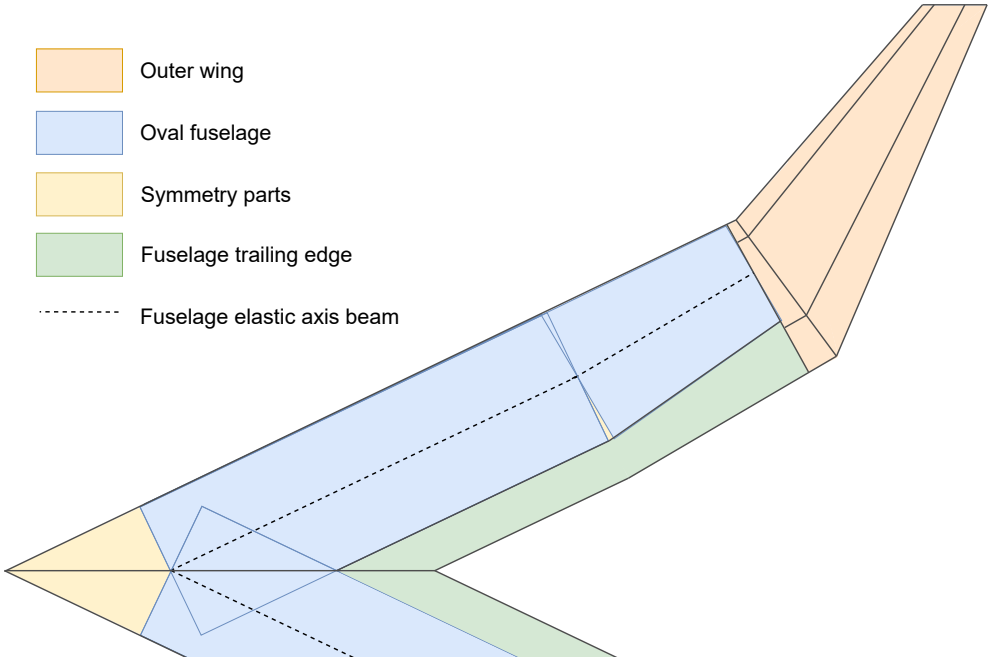

Fig. 6 Weight estimation methods applied to estimate the wing and fuselage weight of the Flying-V.

The structure weight of the Flying V, $W_{\text{structure}}$, is divided in three parts Equation 6:

$$W_{\text{structure}} = W_{\text{fins}} + W_{\text{outer wing}} + W_{\text{fuselage}} \tag{6}$$

The weight of the fins, W_{fins}, is estimated using the relation for vertical tail weight of Torenbeek. The weight of the outer wing, $W_{\text{outer wing}}$, is estimated using EMWET [15]. EMWET is a method that allows quick calculation of

aircraft wing weight based on the loads acting on the wing, including both aerodynamic loads (AVL) and inertial loads resulting from the airframe, payload, and fuel. It computes the weight of the stiffened shell elements of the wing box using the equivalent-plate assumption. Load cases include (trimmed) +2.5g maneuvers at maximum take-off weight and maximum zero-fuel weight. Empirical correlation factors are used to size the secondary-structure weight and nonstructural weights according to the work of Elham [15].

The structure weight of the fuselage, W_{fuselage}, comprises the weight of the primary structure, the weight of the fuselage trailing edge (green in Figure 6) and the weight of additional secondary structure:

$$W_{\text{fuselage}} = 0.8\left(1.5W_{\text{primary}} + W_{\text{fus}_{\text{TE}}}\right) + W_{\text{additional secondary}} \tag{7}$$

The primary weight of the oval fuselage, W_{primary}, is estimated using the method of Schmidt as the principal method to build upon [16]. The fuselage trailing-edge weight $W_{\text{fus}_{\text{TE}}}$ is estimated using an equation of Torenbeek [13]. This relation has been used by e.g. Vos et al. to estimate the trailing edge weight which completes the aerodynamic shape of a BWB aircraft [14]. Additional secondary weights such as for the cockpit, bulkheads and cargo doors, weight estimates by Howe [17] are employed. While originally designated for blended-wing body aircraft[18] [19], it is deemed that these estimations would also be appropriate for the Flying V. The factor 1.5 accounts for a weight increase due non-ideal structures in line with estimations of Droegkamp mentioning an increase of 1.25 to 2.5 [20]. The weight of the outer wing, fuselage trailing edge and fins is reduced by 20% to account for the use of composite materials instead of metals [21]. Hence, the factor 0.8 in Eq. 7.

To compute the primary weight of the fuselage, the fuselage is modeled as an Euler-Bernoulli beam residing at the center axis of the fuselage, as shown in Fig. 6. Along this beam, the fuselage is discretized into perpendicular sections. Moments introduced within the beam due to the slight kink in the center axis beam at the start of the tapered cabin section are neglected; only the bending moment, torsion and shear force are considered. For each section, the longitudinal, lateral, transverse and pressure loads are calculated for ten load cases, as described in Table 1. In all these cases, the aircraft is assumed to be fully loaded with passengers. The maximum and minimum load factor are 2.5 and -1.0, respectively. For both landing load cases, the landing gear struts exert a point load on the aircraft resulting from a hard landing. The landing gear is assumed to provide 50% of the total upward force [22], while the remaining force is assumed to come from the lift on the wing. As such, at a load factor of 2.5 this would mean that the landing gear has to withstand 125% of the takeoff weight, with the remaining 125% of the upward force provided by the aerodynamic forces. In all cases, a safety factor of 1.5 is applied.

Table 1 Load cases considered for the Flying-V and reference aircraft.

Load case	Fuel mass	Pressurization	Load factor
1	Max	Max	+2.5g
2	Min	Max	+2.5g
3	Max	Max	-1.0g
4	Min	Max	-1.0g
5	Max	0	+2.5g
6	Min	0	+2.5g
7	Max	0	-1.0g
8	Min	0	-1.0g
9	Max	0	+2.5g, landing
10	Min	0	+2.5g, landing

After all loads during these scenarios has been determined, the thickness of the various components is estimated based on different criteria to prevent the structural elements from failing, including the Von Mises yield criterion for bi-axial loading. Failure criteria for the beams of the trapezoidal structure are dimpling, crimping, wrinkling and global buckling. Criteria for the stiffened outer skin are global buckling and the critical buckling load. The interested reader is referred to the article of Schmidt and Vos for an extensive description [16] of the failure criteria that are considered. For the present work, this method has been further extended to allow the torsional loads stemming from the outer wing to be introduced. This extension is presented in Appendix A.

The center of gravity of the aircraft is determined from the weight and location of all component weight groups. The weights are either point loads or distributed loads. Passengers, furnishing and operational items are assumed to be linearly distributed over the length of the passenger cabin. The passenger cabin starts at the root of the fuselage beam. Its end point is determined based on the total floor area the passengers and furnishing require. The weight of the systems, secondary weights and fuselage trailing edge is linearly distributed over the length of the fuselage. The structural weight of the fuselage and inner wing is computed per section and is distributed accordingly. The longitudinal location of the main landing gear is determined based on the most aft centre of gravity location, placing the landing gear strut at an angle of 17 degrees. As such a maximum pitch angle of 17 degrees can be achieved at the most aft center of gravity [12]. The length of the landing gear strut and the diameter of the landing gear tires are obtained from Bourget for a floor height of 5.5 m. Hence, $L_{\mathrm{LG_{strut}}}$ is 5.5 m and $r_{\mathrm{LG_{wheel}}}$ is 0.635 m. The longitudinal location of the nose landing gear is assumed to be fixed at the root of the fuselage beam.

D. Fuel Burn Analysis

The fuel weight is estimated using the fuel fraction method. For most flight segments, the fuel fractions for transport jets provided by Roskam are used [23]. 5% reserve fuel is included to account for the diversion and loiter phases [24]. Taxiing and shutdown can be done using the reserve fuel. As such, the fuel fractions of these flight segments are not included in the total mission fuel weight.

For the cruise segment, the Breguet range equation is used to calculate the fuel fraction, described in Equation 8 [25]:

$$R = \frac{V}{c_T}\frac{C_L}{C_D}\ln\left(\frac{W_{\text{start of cruise}}}{W_{\text{end of cruise}}}\right) \tag{8}$$

Here, the flight velocity V follows from the cruise Mach number:

$$V = M \cdot a = M \cdot \sqrt{\gamma RT} \tag{9}$$

The specific fuel consumption c_T is assumed to be 14.0 N/N/s, which is slightly higher than 13.5 N/N/s claimed on Wikipedia[¶] to account for non-ideal conditions during cruise, since engines often not continuously operate at their optimal design condition. The static temperature T follows from the cruise altitude, the atmospheric temperature lapse rate and the atmospheric temperature of 288.15 K at zero altitude. The atmospheric temperature lapse rate is $6.5 \cdot 10^{-3}$ K/m until an altitude of 11,000 m and above this altitude the temperature is constant until an altitude of 20,000 m. γ is the heat capacity ratio, which is 1.4 in dry air, and R is the specific gas constant which is 287 J/kg/K in air.

Equation 8 is also used to determine the range at maximum structural payload as well as the ferry range of an aircraft such that the payload-range diagram can be constructed. For these computations the same velocity, specific fuel consumption and lift-to-drag ratio as are used as for the design range.

E. Optimization

The objective of the optimization of an aircraft family is to minimise the weighted fuel burn of the aircraft family members including a penalty p for any violated constraint:

$$\min f(\bar{x}) = \min_{\bar{x}} \sum_{i}^{N} \frac{W_{\mathrm{fuel}_i}(\bar{x})}{W_{\mathrm{fuel}_{i_0}}} + p(\bar{x}) \tag{10}$$

where $\bar{x}$ is the design vector that describes the aircraft planform as well as the cross section at sections 1 and 3 (see Fig. 5). Table 2 shows the design variables in the top row along with the initial values for the three aircraft variants of the Flying V (FV) denoted with the values -800, -900, and -1000. The constraint penalty function is programmed in such a way that whenever a constraint is violated, a high value is computed by $p(\bar{x})$.

The optimisation algorithm used to perform the smaller optimisation steps within the larger optimisation procedure is the Differential Evolution (DE) algorithm, implemented in SciPy[‖] and described by Storn and Price [9]. The differential evolution algorithm constructs a variety of design vectors and selects the most promising design vectors to be the seed of a new generation. This algorithm is capable of finding the global optimum. In each optimization step, the 10% most promising design vectors in terms of fuel burn are selected, followed by a selection of the design vector with the smallest center of gravity shift during flight.

[¶] `https://en.wikipedia.org/wiki/Rolls-Royce_Trent` [cited on 24-3-2021]

[‖] `https://docs.scipy.org/doc/scipy/reference/generated/scipy.optimize.differential_evolution.html` [cited on 26-11-2020]

Table 2 Design variables and initial values for the optimization of the Flying V. The only unique variable for every aircraft variant is the length of the untapered cabin L_1.

	L_1	L_3	b_{outer}	λ	c'_1	c'_3	H_{1_1}	H_{1_3}	H_{3_1}	H_{3_3}
FV-800	18.75									
FV-900	23.75	11.1	15.33	0.15	1.16	1.21	0.6	0.6	0.7	0.6
FV-1000	28.75									

III. Verification and Validation

In this section, a verification of the described methods is performed and the results are validated. The aerodynamic analysis and weight estimation method will be verified and validated first, followed by a validation of the resulting fuel burn performance.

A. Aerodynamic Analysis

The aerodynamic characteristics of a Flying-V design approximating the design of Faggiano [4] are assessed. Variable values are presented in Table 3. AVL is run in the subsonic incompressible regime for the described aircraft.

Table 3 Fixed and design variables for the approximation of Faggiano's Flying-V geometry [4]. Fixed variables are further explained in Table 14.

L_4	w_{H_1}	w_{H_3}	H_{2_1}	H_{2_3}	H_{arm_3}	L_1	L_3	b_{outer}	λ	c'_1	c'_3	H_{1_1}	H_{1_3}	H_{3_1}	H_{3_3}
11.0	5.97	3.3	2.1	1.8	0.05	21.5	7.0	15.3	0.15	1.25	1.8	0.6	0.3	0.7	0.3
m	m	m	m	m	m	m	m	m	-	-	-	m	m	m	m

Figure 7 shows the drag coefficient and lift-to-drag ratio for a range of lift coefficients. The results obtained with AVL are compared to the results of Faggiano et al. [4]. Clearly, the AVL model closely resembles the results of Faggiano which were obtained using SU2 employing the Euler equations at Mach 0.85. Based on this, the predicted lift-to-drag ratio is considered to be validated.

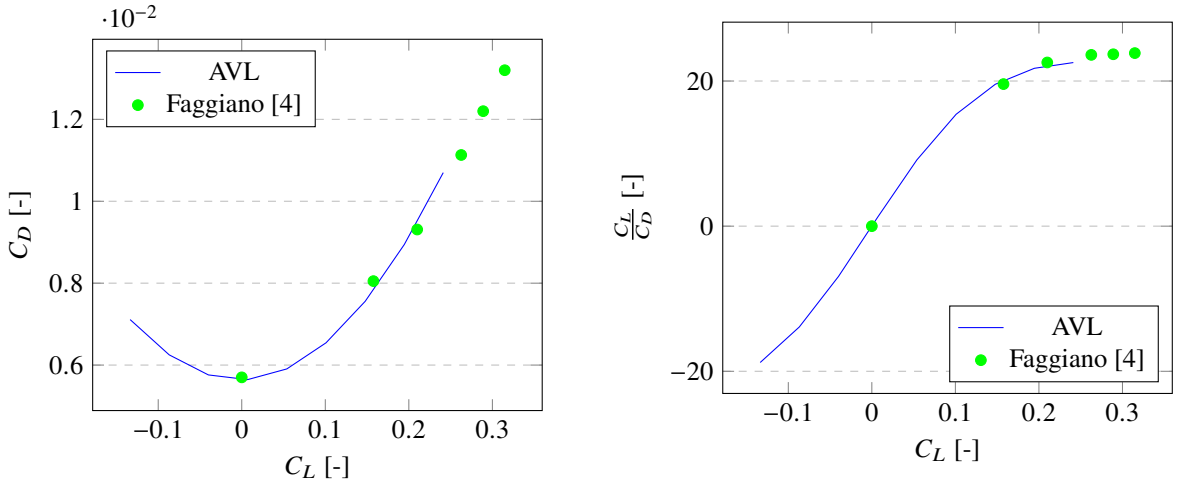

Fig. 7 Validation of the lift-to-drag ratio resulting from AVL with the results of Faggiano et al. [4].

The spanwise lift distribution is an important input to the weight estimation method. At the design lift coefficient, the spanwise lift distribution is assessed using AVL and compared to the results of Faggiano et al. [4], as shown in Fig. 8. In this figure, c_l and c are the local lift coefficient and chord, and c_{ref} is the reference chord of the wing. The untrimmed results of AVL show the lift to be too far outboard. The trimmed results of AVL are obtained by trimming

the aircraft at the same pitching moment coefficient about the moment reference point as Faggiano, resulting in a similar lift distribution that is deemed sufficiently accurate for load estimations.

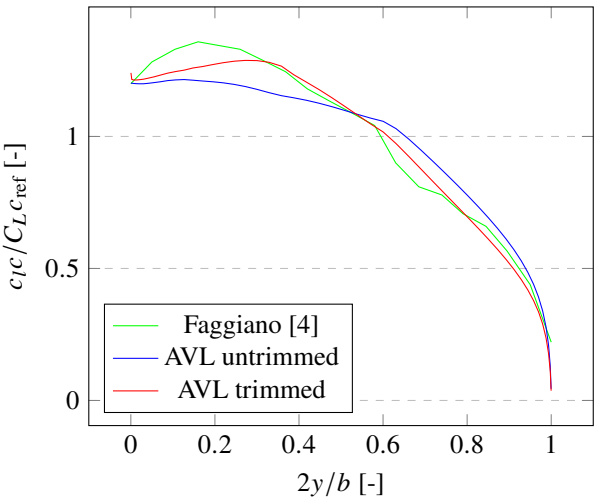

Fig. 8 Spanwise lift distribution at the design lift coefficient. The trimmed AVL results are trimmed at the same pitching moment coefficient as the results of Faggiano et al. [4].

B. Weight Estimation Method

Before diving into the verification and validation of the weight estimation, it should be noted that parts of the model are already considered verified and validated. First of all, the method of Schmidt to estimate the weight of an oval fuselage has already extensively validated by Schmidt [22] and is further elaborated upon by subsequent studies such as by Elmendorp [26]. The empirical relations by Torenbeek form the basis of many aircraft design studies and do not require a very extensive validation. Finally, EMWET is considered to be verified and validated, both by the initial study of Elham and by multiple studies employing this model [15, 26].

Verification and validation of the weight estimation method is performed in two ways. First of all, the A350 reference aircraft has been modeled and its component group weights are compared to earlier studies on the Flying-V and where possible to existing information from Airbus. Secondly, the Flying-V component group weights are compared to the results by Claeys [27]. Performing these two subsequent steps ensures a complete validation of the model,i.e. validating the model including the described oval fuselage weight estimation method both on an existing conventional aircraft with a circular fuselage and on the Flying-V with its oval fuselage.

1. Validation of the Weight Estimation Method for the Reference Aircraft

The reference aircraft that is considered is inspired by the Airbus A350-900. The weight estimation method of Section II.C is employed including the physics-based weight estimations for wing and fuselage. Obviously, the weight estimation for the reference aircraft also includes the empennage and excludes the winglets and fuselage trailing edge. Empennage weight is estimated using the empirical relation of Torenbeek [28]. The weight and aerodynamic loads of the tail surfaces are introduced at their respective half-chord location. Regarding the fuselage weight estimation method, it is assumed that there is no torsion on the fuselage and that the fuselage is not used as a carry-through structure for the wing, meaning that the wing forces are only introduced as a longitudinal load and bending moment on the fuselage beam. The bending moment from the wing structure results from the wing weight (including engine and fuel weight) and aerodynamic loads. The bending moment is calculated with respect to the center of the two wing spars. The weight of the complete wing is estimated using EMWET. The fuel is placed between the spars of the wing, which are placed at 15% and 65% of the chord. Dimensions of the A350-900 are used from Ref. [29].

Component group weights of the reference aircraft are validated using data from Roskam of existing aircraft, as shown in Fig. 9 [30]. The ratio between empty weight and gross weight as well as wing weight and gross weight follows trends of reference aircraft. Note that only the empty weight and wing weight are shown, but that all other component group weights have also been validated.

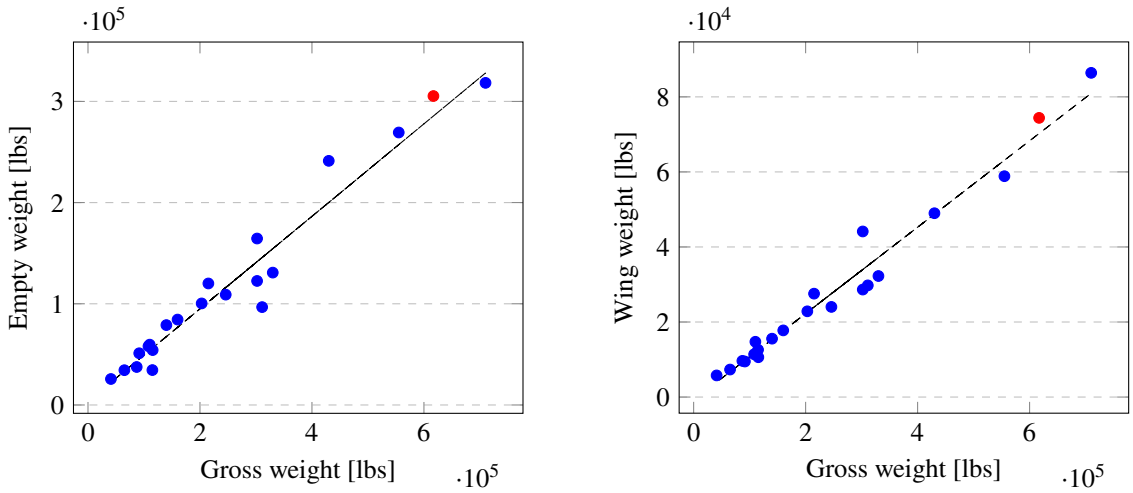

Fig. 9 Empty weight and wing weight validation for the reference aircraft, data from Roskam [30]. Data of the reference aircraft is shown in red, data of Roskam in blue.

A version of the reference aircraft is also modeled by Claeys, modeling a version with a smaller take-off weight to compare to a Flying-V (FV) with the same take-off weight [27]. Claeys sized the structure of the Flying V using an off-the-shelf finite-element method and considered 24 different load cases including the ten load cases considered in the present weight estimation method. Component group weights as a fraction of the operating empty weight (OEW) are compared in Table 4. The largest differences in weights are found in the landing gear and fuselage weight, which can be explained by the lower design take-off weight of Claeys. Additionally, Claeys uses a very high payload weight compared to the structural weight of the reference aircraft, which does not resemble the ratio between payload and OEW reported by Airbus [29]. Furthermore, the empennage weight in the modeled reference aircraft is higher than the results of Claeys, with a very low empennage weight for the study of Claeys. The ratio between weight and surface area of the modeled empennage is 5.1 lbs/m^2. A comparison with data from Roskam [30] shows that this ratio is already relatively low compared to reference aircraft, hence the result of this study is deemed more realistic than the result of Claeys.

Table 4 Component weight groups as fraction of the operating empty weight compared to the results of Claeys [27]. All results are for the -900 aircraft variant. Landing gear is abbreviated as LG and A359 refers to the Airbus to the Airbus A350-900, which is used for reference.

	LG $\frac{W_{LG}}{W_{OEW}}$	Propulsion $\frac{W_{propulsion}}{W_{OEW}}$	Operational items and furniture $\frac{W_{oper\ items}+W_{furniture}}{W_{OEW}}$	Systems $\frac{W_{systems}}{W_{OEW}}$	Wing $\frac{W_{wing}}{W_{OEW}}$	Fuselage $\frac{W_{fuselage}}{W_{OEW}}$	Empennage $\frac{W_{empennage}}{W_{OEW}}$
A359 Claeys	0.12	0.18	0.15	0.12	0.23	0.18	0.02
A359 Present model	0.08	0.17	0.15	0.09	0.24	0.23	0.04
FV Claeys	0.12	0.19	0.15	0.12		0.43	
FV Present model	0.08	0.17	0.17	0.10		0.47	

In conclusion, the comparison studies described in the previous paragraphs show that the semi-analytical, semi-empirical weight estimation method give an acceptable prediction of weight components of the reference airplane. Whether it can also be used with confidence to predict the weight of the Flying V is discussed next.

2. Validation of the Weight Estimation Method for the Flying-V

We will now demonstrate that the same weight estimation method that is used for the reference aircraft can also be used for the Flying V, albeit with completely different input to the geometrical parameters. The starting point is a Flying-V (FV) design that is largely based on the FV-900 design of Hillen [10]. Table 5 describes the design variables of this

Flying-V.

Table 5 Design variables for the Flying V-900 that are used for weight estimation validation.

Variable	L_1	L_3	b_{outer}	λ	c'_1	c'_3	H_{1_1}	H_{1_3}	H_{3_1}	H_{3_3}
Value	23.75	11.1	14.85	0.15	1.16	1.21	0.6	0.6	0.7	0.6
Unit	m	m	m	-	-	-	m	m	m	m

The component group weights of the Flying-V are validated by comparing them to both the reference aircraft and the results of Claeys [27], which are also reported in Table 4. It can be seen that the component group weights, as percentage of the operating empty weight, are rather similar between this study and the results of Claeys. The largest difference for these component group weights is in landing gear weight, which is the result of a lower maximum takeoff weight in this study for the Flying-V such that the landing gear weight can be reduced. The same line of reasoning applies to the weight of the propulsion group. Claeys does not capture this effect and uses the same landing gear on the reference and Flying-V aircraft.

The landing gear of the Flying-V is relatively long compared to reference aircraft [12] and therefore the validity of the empirical relation used to estimate this weight deserves further attention. Bourget studied the landing gear of the Flying-V, considering several options for landing gear design and location [12]. The weight of the landing gear is at 10.0 tonnes for the FV-900 to 11.6 tonnes for the FV-1000, close to the values of Bourget, who obtains 9.7 tonnes to 10.2 tonnes for a 260-tonne MTOW aircraft.

Claeys shows a 17% reduction in primary structural weight between the Flying-V and the Airbus A350. Since EMWET is used to size both the outer wing of the Flying-V and the main wing of the A350 in this study and does not separately output primary and secondary weights, it is not possible to separate the results of this study into primary and secondary weights. The total structural weight (including secondary weights) is reduced by 16% in this research, which is very close to the primary structural weight reduction of Claeys.

The engine location corresponds with the result of Rubio Pascual and Vos, both placing it at 14% of the semispan [31]. The location of the nose and main landing gear for the FV-900 is at at 16.8% and 58.0% of the aircraft length measured from the nose respectively, which closely resembles the results of Bourget placing the gears at 12.6% and 58% respectively [12]. The nose gear could easily be placed more forward, but is currently set at the root of the fuselage center beam. Since the fuselage weight estimation method already includes the assumption to place all weights on the elastic axis of the fuselage, the assumption to place the landing gear placement on this axis does not introduce an additional assumption.

The FV-900 model in this research results in the center of gravity at 27.9 m at the design maximum takeoff weight condition, which is at 52.8 % of the aircraft length measured from the nose of the aircraft. This is very similar to earlier studies on the Flying-V scale model, placing the center of gravity at 52.4%, 52.8-55.9% and 51.8-55.0% of the aircraft length for a 4.6% scaled Flying-V model [32–34].

These comparison studies show that the weight estimation method that is proposed in this study predicts the structural weight of the Flying V just as good as the higher-fidelity method. Furthermore, as this method is also applied to the reference aircraft, it is a deemed a good method to be used in a comparison study between the two aircraft.

C. Fuel Burn Analysis

Verification and validation of the fuel burn analysis is performed in two ways. First of all, the payload range diagram of the reference aircraft is compared to the official data provided by Airbus and the fuel burn for the Flying-V is compared to the reference aircraft and to the studies of Faggiano et al. [4] and Benad [3]. Secondly, a sensitivity analysis on several key input parameters is performed.

Airbus provides the payload-range diagrams of the A350-900 and -1000 reference aircraft, which are compared to the result of this study in Fig. 10 [29]. Since the design mission is at the maximum range with a fully filled aircraft in terms of passengers, these points exactly correlate for all aircraft. It should be noted that these results are for individual aircraft without a commonality constraint applied. Clearly, the modeled reference aircraft closely follow the payload-range specifications of Airbus. The harmonic range of the modeled A350-1000 aircraft is slightly smaller due to a slightly lower maximum takeoff weight. As such, the ferry range for the modeled A350-1000 aircraft is slightly larger than specified.

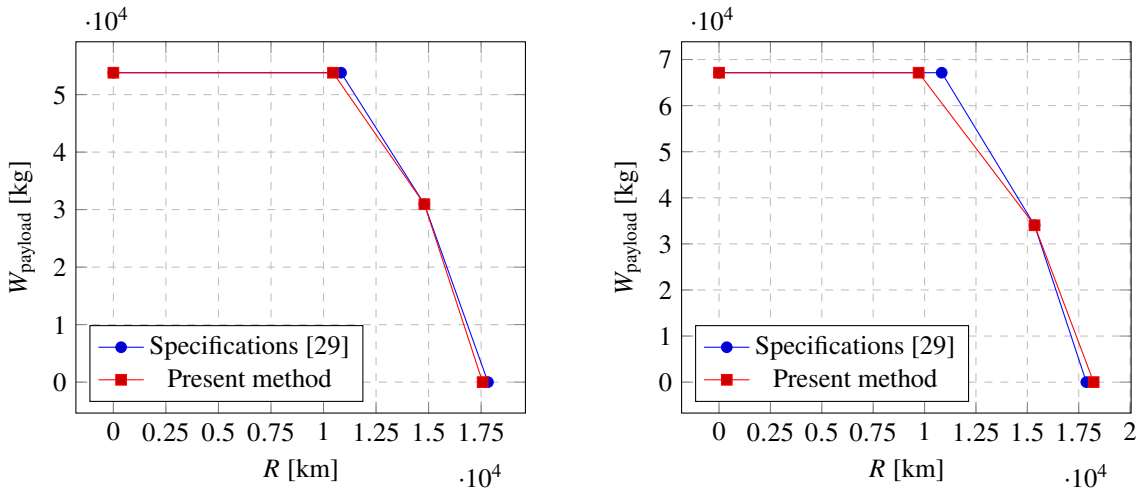

Fig. 10 Payload range diagram of the -900 and -1000 aircraft family members. A350 specifications data from Airbus [29].

The studies of Benad and Faggiano et al. suggest a fuel burn reduction of 20% based on a lift-to-drag ratio improvement of 10% with respect to the reference aircraft or 25% with respect to the NASA Common Research Model [3, 4]. An estimation of this fuel burn performance is made using the FV-900 design of Hillen for the Flying-V [10], which was used during validation of the weight estimation method described in the previous section. Both the Flying-V design and reference aircraft model do not incorporate commonality constraints. The fuel burn of the FV-900 and A350-900 for the design mission are estimated at 92.6 tonnes and 111 tonnes respectively. Hence, the modeled difference in fuel burn performance between the Flying-V and A350-900 is 17.1%, which is close to the estimations of Benad and Faggiano et al. The difference in fuel burn reduction is probably mainly the result of the differences in Flying-V design between the design of Hillen and the design of Faggiano, especially due to a sudden change in thickness between the inner and outer wing, which appears in the geometry created by Hillen [10]. During optimization of the Flying-V this problem is further analyzed and the resulting design presented in Section IV should lead to the larger fuel burn reduction predicted by earlier studies.

IV. Results and Discussion

In this section, the results of the Flying-V aircraft family design are presented and discussed. As alluded to in the previous sections, three variants are designed: -800, -900, and -1000, inspired by the numbering of the A350 family. This section is structured as follows. First the top-level requirements and assumptions are discussed. Then, the presented method is applied to reverse-engineer the A350 family such that these aircraft can be used in the comparison study with the Flying V. Then, the Flying V family is designed for the same set of top-level requirements as the reverse-engineered A350 family. Comparisons are made between the Flying V family and the A350 family. Finally, the fuel burn penalty resulting from the commonality constraints are computed per family member.

A. Top-level Aircraft Requirements and Design Constraints

The top-level aircraft requirements for the aircraft family members are provided in Table 6. The design mission is defined at a full passenger, without any additional cargo weight. The specifications for the -900 and -1000 aircraft are derived from Airbus A350-900 and -1000 aircraft data [29], whereas the specifications of the -800 are set by the authors. The Flying V has the cargo hold behind the main passenger cabin and therefore uses LD4 containers. They are a bit larger than under-the-floor LD3 containers that are used in the Airbus A350 family. The requirements regarding cabin furnishing and emergency exits are all derived from Ref. [29].

The approach speed for the Flying V family members is derived from the A350 family. The reference A350-900 aircraft falls into the Aircraft Approach Category C with an approach speed of 140 kts, while the A350-1000 falls into the D category with an approach speed of 147 kts [29]. Both values are at maximum landing weight. The landing weight W_{MLW} is set at 76% of the takeoff weight, which is the case for the reference aircraft. The approach speed for the

FV-800 is also constrained at 140 kts. For the Flying-V, the lift coefficient in approach configuration $C_{L_{app}}$ is assumed to be 0.73 for all aircraft family members. This value originates from the -900 baseline configuration which was derived by Bourget [12] assuming a trimmed maximum lift coefficient of 1.10.

Table 6 Top-level requirements for the Flying-V aircraft family. The assumed weight of business and economy class passengers is 102 and 93 kg respectively.

		Variable	Unit	-800	-900	-1000
Design range		R_{des}	km	11,200**	14,800	15,300
Design payload	Business class (55")	$n_{\text{pax}_{\text{bc}}}$	# pax	36	48	52
	Economy class (32")	$n_{\text{pax}_{\text{ec}}}$	# pax	257	280	309
	LD4 containers	n_{LD4}	-	18	24	30
	weight	$W_{\text{payload, des}}$	10^3 kg	27.6	30.4	33.1
Maximum structural payload	weight	$W_{\text{payload, max}}$	10^3 kg	35.7	53.8	67.1
Cruise Mach number		M_{cr}	-	0.85	0.85	0.85
Cabin furnishing	Large galley carts	$n_{\text{large carts}}$	-	35	35	44
	Small galley carts	$n_{\text{small carts}}$	-	0	10	10
	Attendant seats	$n_{\text{attendants}}$	-	8	8	8
	Lavatories	n_{lav}	-	7	9	11
	Closets	n_{closets}	-	2	2	2
Emergency exits	Type-A doors per side	$n_{\text{type-A doors}}$	-	2	2	3
	Type-C doors per side	$n_{\text{type-C doors}}$	-	2	2	1

**The range of the Flying-V -800 is actually not a constraint but follows implicitly from the family optimization procedure based on its available fuel tank volume.

Table 7 lists the constraints that are being used in the optimization procedure. The cabin floor area that is listed per family member is based on preliminary studies of the Flying-V cabin that ensure that the number of passengers can fit on the floor using the seat pitches tabulated in Table 6. Requirements on wingspan, outer main gear wheel span, tail height and approach speed follow from the reference aircraft and requirements on aircraft in Code E/Group V of the FAA and ICAO**. The engines should not be less than 5 m apart as suggested by Rubio Pascual [35] to satisfy disk failure requirements. An overview of all the additional input that has been used in this study is provide in Appendix B.

Table 7 Constraints on the Flying-V (FV) aircraft family.

Description	Constraint			Value			Unit
				FV-800	FV-900	FV-1000	
Approach speed	V_{app}	$\leq$	$V_{\text{app}_{\text{max}}}$	140	140	147	kts
Passenger cabin floor	S_{paxcabin}	$\geq$	$S_{\text{paxcabin}_{\text{req}}}$	242	283	315	m^2
Total cabin floor	$S_{\text{totalcabin}}$	$\geq$	$S_{\text{totalcabin}_{\text{req}}}$	332	405	468	m^2
Wingspan	b	$\leq$	b_{max}		65.0		m
Outer main gear wheel span	y_{mlg}	$\leq$	$y_{\text{mlg}_{\text{max}}}$		14.0		m
Engines lateral distance	y_{eng}	$\geq$	$y_{\text{eng}_{\text{min}}}$		5.0		m
Tail height	h_{tail}	$\leq$	$h_{\text{tail}_{\text{max}}}$		20.1		m
Longitudinal static stability	x_{sm}	$\geq$	$x_{\text{sm}_{\text{min}}}$		0.0		m
Directional static stability	C_{n_β}	$\geq$	$C_{n_{\beta_{\text{min}}}}$		0.0005		1/deg
Lateral static stability	C_{l_β}	$\leq$	$C_{l_{\beta_{\text{max}}}}$		0.0		1/rad

**https://www.skybrary.aero/index.php/ICAO_Aerodrome_Reference_Code [cited on 27-2-2021]

B. Reference Aircraft Family

The reference aircraft family consists of the two members of the A350 family: the -900 and -1000. Using the method of Section II and the relevant data from Tables 6 and 7, the two aircraft family members are designed. The wing and empennage of the A350-900 and A350-1000 are identical, only the length of the fuselage is different. In addition, the landing gear of both aircraft are not assumed to be identical, since this is not the case for the real Airbus A350 either [29].

To create the -1000 version of the aircraft from the -900 version, 7 frames are inserted between the nose and wing and 4 frames are inserted aft of the wing. In Table 8 a comparison is made between the published specifications of the two airplanes and the modeled performance in terms of fuel burn and in terms of MTOW. It can be seen the the differences are on the order of single percent point. The payload-range performance of the resulting aircraft is shown in Figure 12 along with a comparison to the published Airbus specifications [29]. These will be further discussed in subsection IV.C.

Table 8 Fuel burn and MTOW for the reference aircraft, specification data from Airbus [29].

		A350 specifications [29]	A350 family model	Difference %
W_{fuel} [10^3 kg]	-900	113.2	112.2	-0.9
	-1000	127.7	128.4	0.5
MTOW [10^3 kg]	-900	280.0	281.2	0.4
	-1000	316.0	312.3	-1.2

C. Flying-V Family

1. Optimisation Results

All Flying-V aircraft have been optimized both as part of the aircraft family (Family Optimized, FO) and individually (i.e. Single Optmized, SO). For the SO, the process of Fig. 3 is employed, while for the family optmization, the method of Fig. 4 is used.

Table 9 presents the component weights of both the individually optimized aircraft and family-optimized aircraft. It can be seen that the maximum take-off weight for each of the family-optimized aircraft members is larger than the single-optimized value. While the -1000 has only a 7-tonne increase in maximum take-off weight due to the application of the commonality constraint, the -800 has a 14-tonne penalty. This attributed primarily due to a penalty in structural weight, landing gear weight and the increase in fuel. Many of the other weight components (furniture, systems, operational items) are not influenced by the application of the commonality constraint as can be expected. Note that the weight of the propulsion system is not constant between the three variants, due to the assumption that the thrust-to-weight ratio of each airplane is the same.

Table 10 shows the value of some of the constraints and other performance indicators that are evaluated during the optimization. Here it can be seen that the lift-to-drag ratio of each of the family members hovers around 21 in trimmed, mid-cruise condition. The penalty in lift-to-drag ratio due to the application of the commonality constrain ranges between 0.2 and 0.9 depending on the variant. The approach speed constraints of a 140kts for the smallest versions and 147kts for the largest version are not active. During the design mission, the center of gravity shift is rather large for both the SO and FO versions of each family member. The main reason for this is the fact that the passengers are located towards the front of the cabin, whereas the cargo containers are placed aft of the cabin, shifting the center of gravity aft quite significantly. The static margin is relatively large in all cases.

The values of the design variables corresponding to the single-optimized and family-optimized aircraft are presented in Table 11. It can be seen that the taper ratio for both the SO and FO designs tends to the lower bound of 0.10. This reduces the size of the outboard wing, shifting the aerodynamic center further forward, reducing the static margin as well as the trim drag. If we look at the family-optimized design variables, we can see that the dimensions of the tapered cabin are mostly sized by the smallest family member. The difference in L_3 for the -1000 variant between the SO and FO version is 9.0 meters, which indicates the large adaptations that the commonality constraint imposes on the geometry of the airplane variants. The outer cabin crown and keel height H_{1_3} and H_{3_3} are set at 0.45 m, which is the result of a trade-off. On the one hand, the crown and keel height should not be too small to limit the radius of the oval cabin

Table 9 Component group weights in the design condition for the single optimization (SO) and family optimization (FO), all in 10^3 kg.

	FV-800		FV-900		FV-1000	
Weight group	SO	FO	SO	FO	SO	FO
Payload	27.6	27.6	30.9	30.9	34.0	34.0
Fuel	53.3	58.0	81.6	87.5	98.6	103
Landing gear	6.8	11.1	9.2	11.1	10.7	11.1
Propulsion	16.1	16.1	19.6	19.6	21.9	21.9
Operational items	5.2	5.2	5.8	5.8	6.4	6.4
Furniture	12.1	12.2	14.3	14.3	16.6	16.7
Structure	39.2	43.8	51.1	52.4	57.4	60.0
Systems	10.4	10.7	12.2	12.3	13.5	13.4
OEW	89.9	99.9	112	115	127	129
MTOW	171	185	225	234	259	266

Table 10 Key characteristics for the single optimization (SO) and family optimization (FO).

		FV-800		FV-900		FV-1000	
		SO	FO	SO	FO	SO	FO
Static margin	m	2.3	1.9	2.3	2.6	2.7	3.3
Fuel tank volume available	m^3	67	72	101	109	124	133
Fuel tank volume required	m^3	66	72	101	109	123	128
Span	m	57.1	55.5	63.2	60.7	65.0	65.0
Approach speed	m/s	64.4	67.2	67.9	70.1	69.3	70.7
Lift-to-drag ratio	-	21.1	20.9	22.5	21.6	21.7	21.2
CG shift design mission	m	2.4	2.5	2.8	3.0	2.9	3.0

and hence limit stresses in the pressurised cabin. On the other hand, a larger keel or crown height would increase the abrupt change in thickness between the inner and outer wing with possibly negative aerodynamic effects such as flow separation.

Table 11 Design variables for the, single optimisation (SO) and family optimisation (FO) results.

		FV-800		FV-900		FV-1000	
Variable	Unit	SO	FO	SO	FO	SO	FO
L_1	m	17.5	18.0	19.1	24.0	21.0	29.0
L_3	m	12.0	11.0	16.6	11.0	20.0	11.0
b_{outer}	m	15.5	14.8	16.0	14.8	14.2	14.8
λ	-	0.10	0.10	0.10	0.10	0.10	0.10
c'_1	-	1.07	1.11	1.12	1.11	1.14	1.11
c'_3	-	1.12	1.13	1.12	1.13	1.13	1.13
H_{1_1}	m	0.63	0.68	0.65	0.68	0.65	0.68
H_{1_3}	m	0.45	0.45	0.45	0.45	0.45	0.45
H_{3_1}	m	0.64	0.68	0.65	0.68	0.65	0.68
H_{3_3}	m	0.45	0.45	0.45	0.45	0.45	0.45

The length of all plugs is given in Table 12. The lengths of the plugs are not an exact multiple of the frame pitch because the variables describing the Flying-V were defined to be continuous. In reality, the lengths of the plugs should be a multiple of the frame pitch, which is largely determined by the window pitch of the aircraft. The fins resulting from this optimized aircraft family have a maximum height of 5.0 m, which means that the maximum tail height constraint is easily met. The track width of the largest aircraft variant is set at 12.2 m following from the study of Bourget [12], such that the constraint on track width is not active either.

Table 12 Length of fuselage plugs to build a family of Flying-V aircraft.

plug		frames	length (m)
-900	front	4	2.67
	aft	5	3.33
-1000	front	3	1.88
	aft	5	3.12

Figure 11 visualizes one wing half of the Flying V-1000 with the plugs highlighted in green and yellow. The floorplan shows that the envisioned payload and cargo indeed fits on the available floor space. A ten-abreast cabin is proposed with a width of 6.2 m. The fuselage component between the plugs is common to all versions and therefore has the emergency exits, lavatories, landing gear and engine pylon attached. A sectional view shows that the cargo containers could also be fitted albeit with a reduced height of the seven most outboard containers to limit the thickness-to-chord ratio of the outboard wing. Two out of the four Type A doors on either side are located side-by-side connected to a cross aisle to ensure emergency evacuation can be performed withing 90 seconds.[††]

The payload-range diagrams of the optimized Flying-V aircraft family members are compared to the reference aircraft family in Figure 12. The FV-900 and FV-1000 have a lower empty weight and maximum takeoff weight than their competitor such that the harmonic range is smaller and the ferry range is larger. However, it can be seen that the design missions can be performed as expected. The FV-800 does not have an A350 reference aircraft to compare with. The FV-800 is constrained in fuel volume, giving it a much smaller range than the -900 and -1000.

[††]See study by Gebauer, J. and Benad, J., "Flying V and Reference Aircraft Evacuation Simulation and Comparison," `https://www.researchgate.net/publication/349309406_Flying_V_and_Reference_Aircraft_Evacuation_Simulation_and_Comparison`, accessed 30 March 2022.

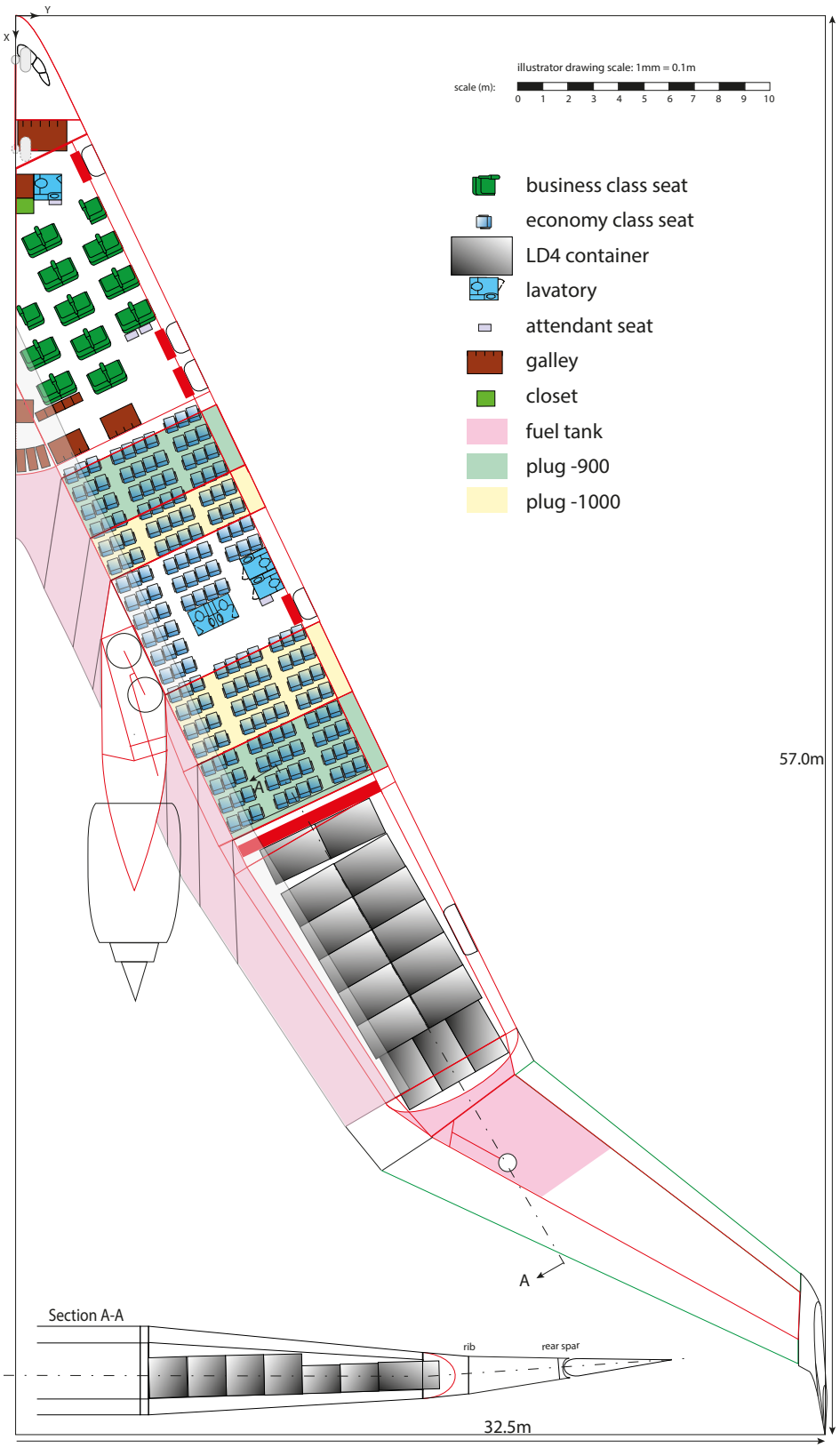

Fig. 11 Floor plan of the FV-1000 aircraft, visualising the plugs to form a FV-800 or FV-900 variant. Note that the floor plan of the cabin is not symmetric. Business class seats (55" pitch): 52, economy class seats (32" pitch): 309, total: 361.

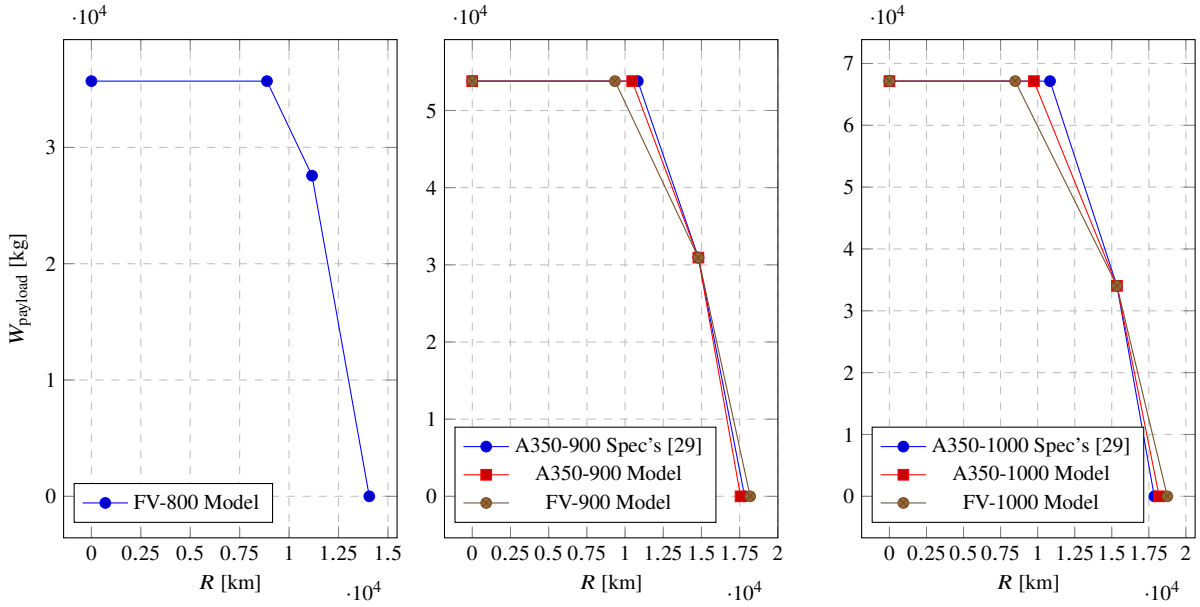

Fig. 12 Payload range diagram of the -800, -900 and -1000 aircraft family members. A350 specifications (spec's) data from Airbus [29].

2. Driving Requirements in Flying-V Family Design

There are several driving requirements in the optimized Flying-V family. Naturally, the most important active constraint is the commonality in design variables and components between the different aircraft variants. Several other top-level requirements are discussed in this section.

As expected, requirements on the volume and floor area of the payload are driving. Sufficient floor area for the passengers should be available with a minimum cabin height towards the back of the cabin of 1.9 m. Since the length of the tapered cabin is set at a maximum of 11 m by the smallest member, the minimum cabin height is not an active constraint. The total floor area of the cargo, passengers, lavatories, galleys and free space for aisles is an active constraint in all family members. The fuel volume is also an active constraint in the optimized aircraft family, in which only the fuel tank of the largest aircraft variant is not completely filled in the design condition.

The constraint on the span is also active during the optimization. The maximum wingspan of 65 m means that the outer wing can have a maximum length of 14.8 m following from the span constraint on the largest aircraft variant. As such, the smaller aircraft variants have a limited total wingspan whereas the individual aircraft optimizations show a somewhat larger wingspan is preferable for these variants (see Table 11). Naturally, removing the commonality constraint on the outer wing would allow for unique outer wingspans between aircraft variants.

The center-of-gravity shift during flight is a driving requirement in the optimization of the aircraft family. As explained in Section II, a constraint on the center of gravity shift is hard to define, and hence it is included implicitly in the optimization procedure.

Constraints that are not active are the constraints on the approach speed, tail height, main gear track width and directional and lateral static stability. The constraint on approach speed entails an assumption on the (trimmed) lift coefficient during approach, which is in turn is derived from the trimmed maximum lift coefficient. Further research is required to check the validity of this assumption, but since the approach speed of the optimized Flying-V family is quite low (70 m/s $\approx$137kts), a small decrease in maximum lift coefficient would still not activate the approach speed requirement. The constraint on tail height is also easily met, allowing an increase in tail height of approximately 3 m with respect to the optimized family design and earlier Flying-V designs. The main gear track width for the largest Flying-V variant is 12.2 m, a margin of 1.8 is present with respect to the maximum track width of 14 m. AVL suggests that the aircraft are all directionally stable. A more sophisticated aerodynamic model should be used to verify these stability derivatives in later design phases as the zero-thickness assumption is of AVL is known to give a poor prediction of the directional stability.

3. Discussion: Cost of Commonality

A comparison between the results for a single-optimized (SO) aircraft with the family optimized aircraft yield the component commonality penalty. Looking at the last row of Table 9, the increase in takeoff weight is 8.1%, 4.0% and 2.7% for the -800, -900 and -1000 respectively. This is primarily the result of a larger structural weight and landing gear weight. The landing gear weight increases significantly for the -800 and -900 version by 62% and 18% respectively. For the -800 version this would be a good motivation to review the landing-gear design and select smaller wheels, brakes and maybe even a shorter strut. However, this is not taken into account in this study.

The penalty in fuel burn for the design missions is approximately 8.8%, 7.2% and 4.4% for the -800, -900 and -1000 respectively (second row of Table 9). The relatively large increase in fuel weight for the -800 and -900 aircraft can be mainly explained by the large increase in landing gear weight which comes with an increase in structural weight. For the -900 a shift in forward shift in the center-of-gravity also increases the static margin. An increase in static margin has a negative effect on the lift-to-drag ratio, resulting from larger elevon deflections to trim the aircraft. The center of gravity is shifted forward in the family-optimized aircraft mainly due to the more forward location of the fuel and increased fuel weight. The fuel is located more forward due to the constraint on the length of the tapered cabin part. Note that this center of gravity location is at the design weight with full fuel tanks. During flight the center of gravity can be shifted aft by pumping fuel aft. This will be considered in a follow-up study. Also the family-optimized -1000 suffers from the implications of a larger static margin than its single-optimized counterpart. In addition, the non-optimal value of the design parameters also contributes to the 4.4% higher fuel burn.

D. Comparing the Flying-V and Reference Aircraft Families

The fuel burn of the reference aircraft family following from the model and as specified by Airbus has already been presented in Table 8. A measure for the payload-range performance Payload Range Efficiency (PRE), defined by Nangia as [36]:

$$\text{PRE} = \frac{W_{\text{payload}} \cdot R}{W_{\text{fuel}}} \tag{11}$$

The payload-range efficiency of the Flying-V and reference aircraft is assessed at the harmonic range and design range and tabulated in Table 13. Also the fuel used per seat per 100 km is added for the design mission along with other figures of merit. Clearly, the payload-range efficiency of the Flying-V is higher than the reference aircraft, especially at the design mission. The fuel burn in liters per seat per 100km also shows this: a 23% and 20% reduction for the -900 and -1000, respectively. The lower fuel burn stems from two sources: the higher glide ratio ($left(C_L/C_D\right)$) and the lower maximum take-off weight. The harmonic range of the Flying-V is somewhat limited due to its relatively low maximum takeoff weight, such that the difference in PRE is less pronounced for the maximum-payload mission.

Table 13 Performance characteristics for the reference aircraft family and optimized Flying-V family. Airbus A350 approach speed data from Airbus [29].

	Unit	FV-800	FV-900	A350-900	FV-1000	A350-1000
$W_{\text{fuel}_{\text{des}}}$	10^3 kg	58.0	87.5	112	103	128
$\text{PRE}_{\text{harmonic}}$	10^3 km	5.47	5.75	5.02	5.54	5.10
PRE_{des}	10^3 km	5.30	5.23	4.08	5.09	4.07
$(V_F/\text{seat}/100\text{km})_{\text{des}}$	liter	2.21	2.18	2.83	2.24	2.80
$(C_L/C_D)_{\text{des}}$	-	20.9	21.6	19.7	21.2	19.5
MTOW	10^3 kg	185	234	281	266	312
W/S	kg/m^2	271	295	636	300	673
V_{app}	kts	131	136	140	137	147

The wing loading of the Flying-V, W/S, is much lower than the reference aircraft due to its very large wing area and lower takeoff weight. This directly affects the approach speed of the aircraft, such that the approach speed of the Flying-V is lower than for the reference aircraft. An obvious additional benefit of the Flying-V aircraft family is the automatic scaling of the wing surface area and fuel tank volume with an increase in cabin size. This results in a more constant wing loading between the aircraft family members, such that the approach speed does not differ as much

between aircraft variants as for conventional aircraft. Table 13 shows a relatively small difference in approach speed between the FV-900 and FV-1000, confirming a proportional growth of wing area with landing weight. In conventional aircraft families such as the reference Airbus A350 the wing loading increases for the larger aircraft variants, assuming roughly the same wing is used on all aircraft variants. Hence, a proportional growth of wing area with takeoff weight can be described as a benefit of the Flying-V configuration, indicating that smaller family members are not designed with an oversized wing area.

Comparing the driving requirements in Flying-V family design with a conventional aircraft configuration, it should be noted that the Flying-V copes with difficulties in terms of center of gravity shift during flight and static margin to a higher extent than is expected for a conventional aircraft family. The center of gravity shift for the reference aircraft is described by Bourget as 20% of the MAC, with a 9.1 m MAC, which means a shift of 1.82 m. A 20% MAC shift of the centre of gravity is also indicated by the Flight Deck and Systems Briefing for Pilots by Airbus[‡‡]. Clearly, this shift in center of gravity is much lower than the current FV-900 design (3.0 meter according to Table 10). Since fuel tanks of a conventional aircraft are located mainly in the wing, the increase in fuel volume for a larger aircraft family member is mainly centered around the center of gravity. In addition, the aerodynamic center and center of gravity of a conventional aircraft are relatively close, such that the static margin is generally limited. Furthermore, the addition of extra payload for larger family members can be spread around the center of gravity and the aerodynamic center such that effects on the static margin and center of gravity shift can be limited. Finally, the shift in center of gravity during flight can be kept small when fuel is stored in the wing. For the Flying-V, placing the fuel around the center of gravity means that the fuel is stored mainly along the cabin, whereas the outer wing should not contain a lot of fuel due to its large moment arm with respect to the center of gravity. Employing active center-of-gravity control by pumping fuel along the from the inner tanks to the outer tanks could reduce the static margin during operation. However, this is not taken into account in this research.

V. Conclusion

The goal of this study is to study the design of a family of Flying-V aircraft and to compare its fuel burn performance and driving requirements to a conventional widebody reference aircraft family. A multidisciplinary design optimization for the simultaneous design of three aircraft family members is employed. This method is validated with the A350-900 and A350-1000 aircraft showing differences of 0.9% and 0.5% respectively from the fuel burn specified by Airbus. The fuel burn of the optimized FV-900 and FV-1000 are 22% and 20% lower than their respective Airbus A350 reference aircraft. The optimized Flying-V aircraft family members are compared to individually optimized Flying-V aircraft. The penalty in fuel burn due to common components and commonality in design variables between family members is 8.9%, 7.1% and 4.2% for the FV-800, FV-900 and FV-1000 respectively. The takeoff mass of the Flying-V family members is $185{\cdot}10^3$ kg, $234{\cdot}10^3$ kg and $266{\cdot}10^3$ kg respectively. With respect to the modeled A350 family, this is a reduction of 17% and 15% for the -900 and -1000 variant, respectively. The design ranges of the Flying-V family members at maximum passenger capacity are $11.2{\cdot}10^3$ km, $14.8{\cdot}10^3$ km and $15.4{\cdot}10^3$ km. The range of the FV-800 results from a fuel volume constraint making it considerably shorter than its -900 and -1000 relatives, which have sufficient internal volume to store the required fuel for the design range.

Driving requirements, besides the volume and floor area for the payload and the commonality constraint, are the center of gravity shift during flight, the wingspan of 65 m and the fuel tank volume. The larger aircraft family members can be formed by inserting plugs before and aft of the structural component which has the engine and landing gear attached, inserting 9 frames for the -900 and 8 frames for the -1000, respectively. Wing loading of the Flying-V is approximately 45% lower than for the reference aircraft and is almost constant between the FV-900 and FV-1000, resulting in an estimated approach speed of 136 and 137 kts, lower than the approach speed of 140 and 147 kts of the A350-900 and A350-100, respectively.

Additional research is required to investigate the center of gravity excursion during flight and static margin, combined with the location and size of the fuel tanks. Furthermore, the location and structure of a combined landing gear and engine placement fuselage component deserve further attention, especially coupled with ground stability of the aircraft and aerodynamic efficiency of the proposed engine location. Finally, it will be interesting to study the market prospects of the different Flying-V family members. Excluding one of the three aircraft variants would improve the performance of the remaining aircraft family members, which could lead to the the conclusion that a two-member family is economically more viable than a three-member family.

[‡‡] `http://www.smartcockpit.com/docs/a350-900-flight-deck-and-systems-briefing-for-pilots.pdf` [cited on 6-9-2020]

References

[1] Boas, R., "Commonality in complex product families: Implication of divergence and lifecycle offsets," Ph.D. thesis, Massachusetts institute of technology, 2008.

[2] Liebeck, R. H., "Blended Wing Body design challenges," *AIAA\ICAS International Air and Space Symposium and Exposition: The Next 100 Years*, 2003, pp. 1–13. https://doi.org/10.2514/6.2003-2659.

[3] Benad, J., "the Flying V - a New Aircraft Configuration for Commercial Passenger Transport," *Deutscher Luft- und Raumfahrtkongress*, 2015, pp. 1–8.

[4] Faggiano, F., Vos, R., Baan, M., and Van Dijk, R., "Aerodynamic design of a flying V aircraft," *17th AIAA Aviation Technology, Integration, and Operations Conference: 5-9 June 2017, Denver, Colorado [AIAA 2017-3589] AIAA*, 2017. https://doi.org/10.2514/6.2017-3589.

[5] Willcox, K., and Wakayama, S., "Simultaneous optimization of a multiple-aircraft family," *Journal of Aircraft*, Vol. 40, No. 4, 2003, pp. 616–622. https://doi.org/10.2514/2.3156.

[6] Riaz, A., Guenov, M., and Molina-Cristobal, A., "Set-based approach to passenger aircraft family design," *Journal of Aircraft*, Vol. 54, No. 1, 2017, pp. 310–326. https://doi.org/10.2514/1.C033747.

[7] Messac, A., Martinez, M., and Simpson, T., "Introduction of a product family penalty function using physical programming," *8th Symposium on Multidisciplinary Analysis and Optimization*, 2000. https://doi.org/10.2514/6.2000-4838.

[8] La Rocca, G., "Advanced Engineering Informatics Knowledge based engineering: Between AI and CAD. Review of a language based technology to support engineering design," *Advanced Engineering Informatics*, Vol. 26, No. 2, 2012, pp. 159–179. https://doi.org/10.1016/j.aei.2012.02.002.

[9] Storn, R., and Price, K., "Differential Evolution - A Simple and Efficient Heuristic for Global Optimization over Continuous Spaces," *Journal of Global Optimization*, Vol. 11, 1997, pp. 341–359. https://doi.org/10.1023/A:1008202821328.

[10] Hillen, M., "Parametrisation of the Flying-V Outer Mould Line," Master's thesis, Delft University of Technology, 2020.

[11] Raymer, D., *Aircraft Design: A Conceptual Approach, Second Edition*, American Institute of Aeronautics and Astronautics, Inc., 1998.

[12] Bourget, G., "The effect of landing gear implementation on Flying V aerodynamics , stability and controllability by," Master's thesis, Delft University of Technology, 2020.

[13] Torenbeek, E., "Development and Application of a Comprehensive Design-sensitive Weight Prediction Method for Wing Structures of Transport Category Aircraft," Tech. rep., Delft University of Technology, Delft, 1992.

[14] Vos, R., and Hoogreef, M., "Semi-analytical weight estimation method for fuselages with oval cross-section," *54th AIAA/ASME/ASCE/AHS/ASC Structures, Structural Dynamics, and Materials Conference*, 2013, pp. 1–15. https://doi.org/10.2514/6.2013-1719.

[15] Elham, A., La Rocca, G., and Van Tooren, M., "Development and implementation of an advanced, design-sensitive method for wing weight estimation," *Aerospace Science and Technology*, Vol. 29, No. 1, 2013, pp. 100–113. https://doi.org/10.1016/j.ast.2013.01.012.

[16] Schmidt, R., and Vos, R., "A semi-analytical weight estimation method for oval fuselages in conventional and novel aircraft," *AIAA SciTech Forum - 52nd Aerospace Sciences Meeting*, 2014. https://doi.org/10.2514/6.2014-0026.

[17] Howe, D., "Blended wing body airframe mass prediction," *Proceedings of the Institution of Mechanical Engineers, Part G: Journal of Aerospace Engineering*, Vol. 215, 2001, pp. 319–331. https://doi.org/10.1243/0954410011533329.

[18] Okonkwo, P., "Conceptual design framework for Blended Wing Body aircraft," Ph.D. thesis, Cranfield University, 2016. https://doi.org/10.2514/6.2012-5649.

[19] Brown, M., and Vos, R., "Conceptual design and evaluation of blended-wing-body aircraft," *AIAA Aerospace Sciences Meeting (210059 ed.). [AIAA 2018-0522] AIAA*, 2018. https://doi.org/10.2514/6.2018-0522.

[20] Droegkamp, M., "Finite element model weight estimation," Tech. Rep. 2089, SAWE, 1992.

[21] Soutis, C., "Fibre reinforced composites in aircraft construction," *Progress in Aerospace Sciences*, Vol. 41, No. 2, 2005, pp. 143–151. https://doi.org/10.1016/j.paerosci.2005.02.004.

[22] Schmidt, R., "A Semi-Analytical Weight Estimation Method for Oval Fuselages in Novel Aircraft Configurations," Master's thesis, Delft University of Technology, 2013.

[23] Roskam, J., *Airplane Design Part I - Preliminary Sizing Of Airplanes*, Design, Analysis and Research Corporation, Lawrence, Kansas, 1985.

[24] Faggiano, F., "Aerodynamic design of a flying V aircraft," Master's thesis, Delft University of Technology, 2017.

[25] Ruijgrok, G., *Elements of Airplane Performance*, Delft University Press, 2009.

[26] Elmendorp, R., Vos, R., and La Rocca, G., "A conceptual design and analysis method for conventional and unconventional airplanes," *29th Congress of the International Council of the Aeronautical Sciences, ICAS 2014*, 2014, pp. 1–12.

[27] Claeys, M., "Flying V and Reference Aircraft Structural Analysis and Mass Comparison," Master's thesis, Delft University of Technology, 2018.

[28] Torenbeek, E., *Synthesis of Subsonic Airplane Design*, Delft University Press, 1982.

[29] Airbus, "A350 Aircraft Characteristics Airport and Maintenance Planning," Tech. Rep. Revision No. 8 - May 01/20, Airbus, 2020.

[30] Roskam, J., *Airplane Design Part V - Component Weight Estimation*, Design, Analysis and Research Corporation, Lawrence, Kansas, 1985.

[31] Rubio Pascual, B., and Vos, R., "The Effect of Engine Location on the Aerodynamic Efficiency of a Flying-V Aircraft," *AIAA Scitech 2020 Forum*, 2020. https://doi.org/10.2514/6.2020-1954.

[32] Palermo, M., "The Longitudinal Static Stability and Control Characteristics of a Flying V Scaled Model," Master's thesis, Delft University of Technology, 2019.

[33] Viet, R., "Analysis of the flight characteristics of a highly swept cranked flying wing by means of an experimental test," Master's thesis, Delft University of Technology, 2019.

[34] Ruiz Garcia, A., "Aerodynamic Model Identification of the Flying-V using Wind Tunnel Data," Master's thesis, Delft University of Technology, 2019.

[35] Rubio Pascual, B., "Engine-Airframe Integration for the Flying V," Master's thesis, Delft University of Technology, 2018.

[36] Nangia, R., "Efficiency parameters for modern commercial aircraft," *Aeronautical Journal*, Vol. 110, No. 1110, 2006, pp. 495–510. https://doi.org/10.1017/S0001924000001391.

[37] Megson, T., *Aircraft Structures for Engineering Students*, Aerospace Engineering, Elsevier Science, 2013.

A. Fuselage Weight Estimation

The main difference between the model of Schmidt [16] and the model required for a Flying-V aircraft is the fact that the Flying V has two fuselage barrels that each have a stub wing at the end. The sweep angle of the fuselage means that the aerodynamic moment not only translates into a bending moment, but also in torsion around the center axis of the fuselage. Furthermore, the resultant forces and moments at the root of the outer wing also introduce a torsional moment in the oval fuselage. As such, the model of Schmidt has been enhanced with a torsion model which solves for the shear flows in the cross-section of the fuselage, described in the following section. Furthermore, the fact that there are two fuselages means that the bending moment at the start or root of the fuselage is non-zero, whereas in the BWB configuration of Schmidt et al. the bending moment of the fuselage should be zero both at the first and last section of the fuselage.

The cross-section cells are cut open to calculate the open-section shear flow resulting from the shear force acting on the section. For the described fuselage cross-section, the cuts are shown in the figure, such that only the walls and the floor remain. For a pure vertical shear force and given the symmetric nature of the cross-section, the floor open-section shear flow will also be zero. Hence, only the walls have a non-zero open-section shear flow, which is positive upwards for a positive shear force and will be equal for a symmetrical cross-section. For a given thin-walled cell, the rate of twist is given in Equation 12 [37], in which A_i denotes the area of the cell.

$$\frac{\mathrm{d}\theta}{\mathrm{d}z} = \frac{1}{2A_\mathrm{i}G} \oint_R q \frac{\mathrm{d}s}{t} \tag{12}$$

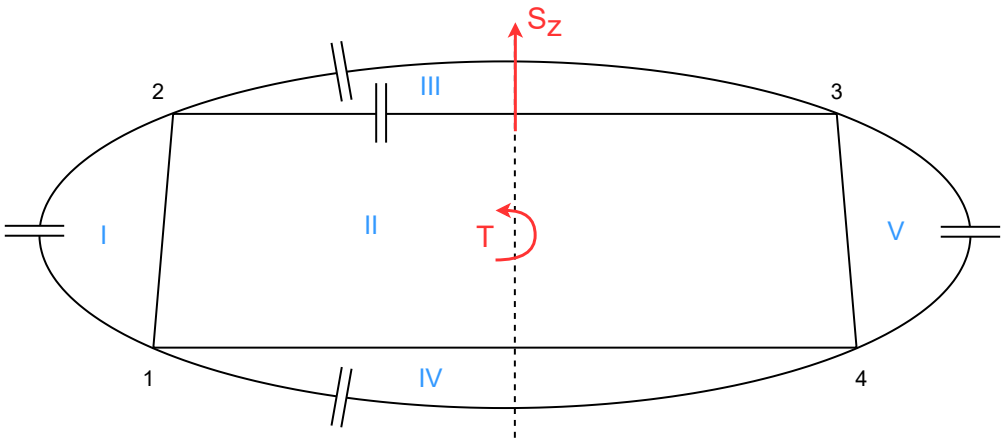

Fig. 13 Oval fuselage cross-section with numbered cells and vertices. Cuts to determine the open-section shear flow are indicated.

The shear flow can be described as the summation of the open-section shear flow and the shear flow at the cuts, which yields a constant shear-flow over the complete cell. As such, Equation 12 can be rewritten into Equation 13 in which the open-section shear flow is denoted by q_{b} and the constant cell shear flow by $q_{\mathrm{s,0,R}}$.

$$\frac{\mathrm{d}\theta}{\mathrm{d}z} = \frac{1}{2A_{\mathrm{i}}G} \oint_R \left(q_{\mathrm{b}} + q_{\mathrm{s,0,R}}\right) \frac{\mathrm{d}s}{t} \tag{13}$$

This equation is evaluated for the fuselage cross-section cells. All shear flows are assumed positive counter-clockwise. Equating the moments at the symmetry axis of the section yields the required sixth equation. Note that the open-section shear flows cancel each other out when the moment is taken around this point, and that the shear force does not contribute either.

$$T = \sum_{R=1}^{\mathrm{N}} 2A_R q_{\mathrm{s,0,R}} \tag{14}$$

Which results in a system of equations which can be solved for the shear flows in the structural members. The shear flow for the front and aft arc and through the walls will not be equal between the front and aft side of the cross-section of the cabin. Since the fuselage weight estimation method assumes a symmetrical cross-section, these loads are averaged between the front and aft side. In reality, this might mean that the front wall needs to have different dimensions than the rear spar.

B. Fixed Variables and Input Values for Optimization Studies

To enable the automatic synthesis process of the reference aircraft and the Flying V family, many constants are applied. For reference, all of these constants are tabulated in Tables 14 and 15. Many of these parameters are explicitly described in the thesis of Hillen [10] and the paper of Schmidt and Vos [16].

Table 14 Constants describing the geometry of the Flying-V. All variables are the same for all aircraft variants.

Description	Variable	Value	Unit
Length between inner and outer wing	L_4	1.0	m
Width at input height of section 1	w_{H_1}	6.2	m
Width at input height of section 3	w_{H_3}	5.8	m
Leading edge sweep of inboard wing	Λ_{in}	64.5	deg
Leading edge sweep of outboard wing	Λ_{out}	40.7	deg
Dihedral angle of trunk 4	Γ_4	-0.1785	deg
Dihedral angle of trunk 5	Γ_5	5.825	deg
Incidence angle of section 4	i_4	0.4	deg
Incidence angle of tip section	i_{tip}	-4.37	deg
Orientation angle of section 4	δ	52.6	deg
Cabin height at section 1	H_{2_1}	2.25	m
Cabin height at section 3	H_{2_3}	1.75	m
Arm-rest height at section 1	H_{arm_1}	0.6	m
Arm-rest height at section 3	H_{arm_3}	0.6	m
Vertical trailing edge position at section 1	z_{TE_1}	-0.3	m
Vertical trailing edge position at section 3	z_{TE_3}	-0.04	m
Upper curve starting location at section 1	$\bar{x}_{s_{\mathrm{up}_1}}$	0.4	-
Upper curve starting location at section 3	$\bar{x}_{s_{\mathrm{up}_3}}$	0.3	-
Lower curve starting location at section 1	$\bar{x}_{s_{\mathrm{low}_1}}$	0.4	-
Lower curve starting location at section 3	$\bar{x}_{s_{\mathrm{low}_3}}$	0.3	-
Upper curve coefficient at section 1	c_{up_1}	$1e^{-5}$	m^{-3}
Upper curve coefficient at section 3	c_{up_3}	$1e^{-5}$	m^{-3}
Lower curve coefficient at section 1	c_{low_1}	$2e^{-3}$	m^{-3}
Lower curve coefficient at section 3	c_{low_3}	$1e^{-4}$	m^{-3}
Upper Bernstein coefficients section 4	A_{u_4}	[0.088, 0.066, 0.21, 0.079, 0.24, 0.23]	-
Lower Bernstein coefficients section 4	A_{l_4}	[-0.13, -0.084, -0.031, -0.31, 0.069, 0.20]	-
Upper Bernstein coefficients section 5	A_{u_5}	[0.14, 0.068, 0.20, 0.078, 0.14, 0.29]	-
Lower Bernstein coefficients section 5	A_{l_5}	[-0.099, -0.084, -0.025, -0.39, 0.061, 0.17]	-

Table 15 Input parameters for the weight estimation method applied in this research, including a reference to a section providing more information on the respective parameter and value.

	Parameter	Unit	Value
Cargo doors	$n_{\text{cargo doors}}$	-	2
Windscreen area	S_{ws}	m^2	2.3
Minimum cabin height	$h_{\text{cabin}_{\text{min}}}$	m	1.9
Number of cycles	n_{flights}	-	100000
Cabin pressure differential	Δp_{cruise}	kPa	57.5
Frame pitch	L_{frame}	m	0.635
Minimum gage thickness	t_{gage}	m	$1.2 \cdot 10^{-3}$
Modelled to actual weight factor	k_{MA}	-	1.2
Safety factor	n_{safety}	-	1.5
Weight reduction metal to composites	k_{MC}	-	0.2
Front spar location outer wing	$\bar{x}_{\text{spar}_{\text{front}}}$	-	0.15
Front spar location outer wing	$\bar{x}_{\text{spar}_{\text{aft}}}$	-	0.60
Spanwise start location fuel tank outer wing	$\bar{y}_{\text{ft}_{\text{start}}}$	-	0.0
Spanwise end location fuel tank outer wing	$\bar{y}_{\text{ft}_{\text{end}}}$	-	0.3
Outer wing rib pitch	s_{rib}	m	0.6
Dive velocity	V_{dive}	m/s	300
Landing gear pitch angle	θ_{LG}	deg	17
Landing gear strut length	$L_{\text{LG}_{\text{strut}}}$	m	5.5
Landing gear wheel radius	$r_{\text{LG}_{\text{wheel}}}$	m	0.635
Number of fuel tanks	n_{ft}	-	4
APU dry weight	W_{apu}	kg	417